Planned Panel Alignment Procedure for the SMA Antennas Using the Microwave Holography Technique

Xiaolei Zhang
Martin Levine
Peter Bratko
John Test
Cosmo Papa
Colin Masson

August 27, 1996

Submillimeter Array Memorandum, No. 85

Original Version: June 14, 1995

Abstract

This memo summarizes the current status of the preparation of the microwave holography system, to be used for the panel alignment of the SMA antennas. Certain optics related issues for the holography experiment are summarized in a separate memo (Zhang 1995). The hardware system, operating at the 90 GHz range, is designed chiefly for the purpose of initial testing at the Haystack site. The system consists of a beacon transmitter operating at 92.4 GHz, two room-temperature receivers, as well as a back-end which uses a Hewlett Packard vector voltmeter as detector. The main receiver operates in the frequency range of 85 - 93 Ghz, which will also serve as the initial system testing/radio pointing receiver at the Haystack site for the first antennas. The phase-reference receiver is in the range of 87-93 GHz, and will be installed at the back of the subreflector, inside the chopper control housing. The back-end down-converts the 2.83 Ghz first IF signals to 21.4 MHz before final detection.

The data acquisition software consists of an X-window user interface on the "gateway computer", which is a SPARC 10; the intermediate communication and averaging software on the antenna computer (a 486); and the low level motion control and data acquisition software in the Programmable Multi Axis Controller (PMAC), which has its A/D converter directly linked to the analog output of the vector voltmeter. The communication between the gateway computer and the antenna computer is done through reflective memory, and the communication between the antenna computer and the PMAC is through the dual-port-RAM. The acquired data is displayed on the gateway computer in real time in the form of color-coded beam map, so that the quality of the acquired data can be monitored. The data is taken "on the fly" with an average rate about 10 points per second.

The analysis software currently implements phase-coherent holography scheme, which employs the Fourier transform technique to recover the aperture phase distribution from the measured antenna beam patterns. Corrections for the near-field effect, large-scale errors, subreflector diffraction, as well as the phase-reference plane determination are incorporated. The algorithm for panel fitting allows the accurate determination of the movement of panels with four adjustable screws. The phase-retrieval algorithms will also be incorporated into the package in the near future.

1 Introduction and General Considerations

The Smithsonian Submillimeter Array (SMA) will be operating in the frequency range of 180 - 900 Ghz, or an equivalent wavelength range of 1.6 mm - 0.3 mm. In order to have an equivalent wavefront phase error of less than $\lambda/20$ for the entire frequency range of operation, a surface rms of about 10 μm is desired, of which 5 μm is allocated for surface measurement and setting.

The microwave holography technique, commonly employed to obtain the antenna aperture (amplitude and phase) distribution from the far field measurement, is well suited for the purpose of fast and accurate measurement of the antenna surface, once the initial alignment of the paraboloid is done using mechanical means. Detailed comparison of the trade-offs of the different surface measurement techniques can be found in the SMA memo No. 50, by Colin Masson (1991).

The holography technique has been employed successfully at most of the radio observatories for reflector surface alignment. The best surface rms obtained so far for the millimeter and submillimeter antennas is about 20 microns. The repeatability of the measurements is about 5 microns. It appears that the goal of aligning the SMA dishes using the holography technique to a surface rms of about 5 - 10 micron is within practical reach.

We have decided to use the traditional "withphase" holography technique during the initial phase of the holography experiment. Phase retrieval methods using either the Misell algorithm (Morris 1985) or the nonlinear least-square global fitting algorithm (Hills & Lasenby 1988) have both been employed in the past to set the surface for single-dish antennas. However, it has been found that the convergence of the Misell algorithm is poor if the initial surface error is large. The solution is often locked onto a local instead of the global minimum of the χ^2 function. The global fitting approach can potentially be superior than the Misell algorithm, if a prior knowledge of the dish error distribution can be properly incorporated into the trial models. At the moment, an appropriate assessment of the accuracy of the phase-retrieval algorithms is still lacking. We have therefore decided to start with the "withphase" approach, using a second receiver which serves as the phase-reference, even before the interferometer array is up and running.

The choice of frequency for the holography beacon transmitter, 92.4 GHz, is selected such that it is outside the protected astronomical band (which is up to 92 GHz) while still low enough so that the entire 85-93 GHz RF band (which includes the SiO maser frequency of 86 GHz) can be covered by a single ZAX Gunn oscillator which has a bandwidth of 4 GHz, with an IF frequency of 2.83 GHz.

At 92.4 GHz, 5 μm of surface error or 10 μm of pathlength error amounts to about 1^o of phase error. The corresponding signal-to-noise needed is about 35 dB. So the thermal noise of the instrument should not be a problem for the beacon source we choose to use, which has an output power about 12 mw (see further the calculation in the next section).

2 Hardware Preparation

2.1 System Layout

In Figure 1, we have plotted the block diagram of the holography data acquisition system. The three configurations are used for observing the terrestrial transmitter, the SiO masers, and the planets and quasars, respectively. The main receiver is used in all three configurations. The phase-reference receiver is used only for the holography test using the transmitter.

At the Haystack site, the transmitter will be mounted on the 200 ft Lowell tower, which is situated about 250 m away from the SMA antenna pads. The main receiver (RCVR 1) is located inside the receiver cabin on the main optical path, near the Cassegrain focus of the antenna dish. The phase-reference receiver (RCVR 2) is located inside the chopping secondary control housing, with the horn looking directly at the transmitting source.

In configuration (a), the signal coupled into the input of the main receiver is about -15 dBm (see the calculation in section 3.2). Due to the difference in collecting area between the main reflector and the reference horn, the two optical paths have a difference in the signal level of about 44 dB after the first mixing. This is compensated by using different amount of amplification for the first IF signal in the two paths. The first IF in the main receiver is amplified by about 20 dB whereas the first IF

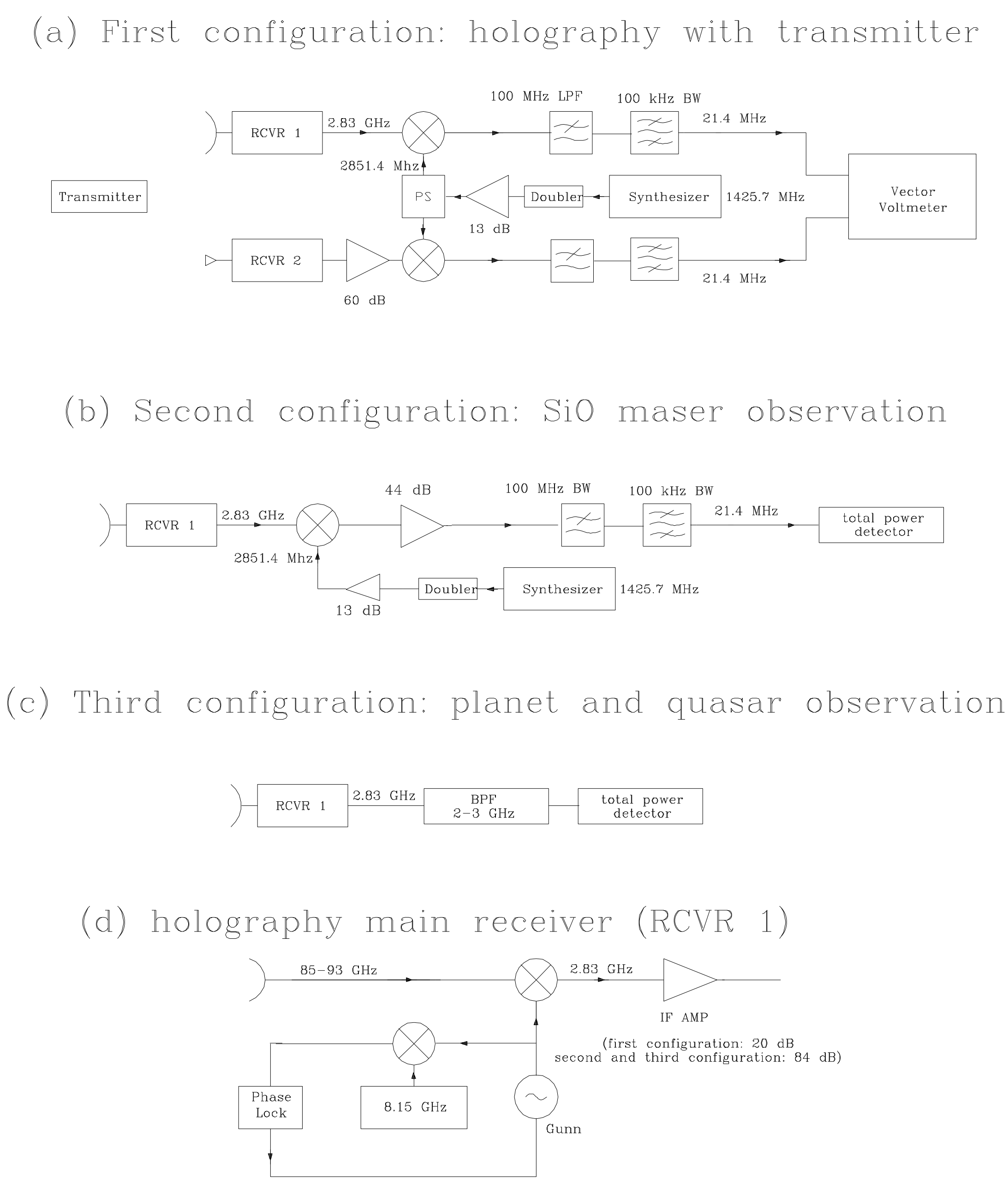

Figure 1: Holography data acquisition system

in the reference receiver is amplified by about 60 dB (the contribution of two 34 dB amplifiers, as well as the loss of the cable leading from the subreflector to the cabin). This way the signal level arriving at the second mixer in the two paths is between -5 dBm to -9 dBm, taking into account of the mixing loss and the losses in the waveguide system.

In configuration (b), for an SiO maser of about 1000 Jy, the signal level at the input of the main receiver is about -140 dBm (for 100 kHz wide line). We plan to use one additional 20 dB and one additional 44 dB amplifier besides the 20 dB amplifier in configurarion 1. Another low frequency amplifier of 44 dB will also be used after the second mixing. This gives a toal signal amplification of 128 dB. Taking into account of mixing loss, etc., the signal level arriving at the second mixer is about -20 dBm.

In configuration (c), for a planet of 500 Jy, the signal level arriving at the input of the main receiver, in an 1 GHz IF bandwidth is -102 dBm. Using a pre-amplification of amount (20+44+20) dB, the signal level just before the BPF is about -25 dBm.

The LO signal for the second mixer is generated from a synthesizer plus doubler arrangement, with a frequency 21.4 MHz above the 2.83 GHz first IF frequency. After the second mixing, the 21.4 MHz signal first passes an 100 MHz low-pass-filter (which provide a bandwidth narrower than the stop-band of the next BPF), and then an 100 kHz band-pass-filter, which determines the ultimate passband in the holography mode, before the final detection at the vector voltmeter.

2.2 Calculations of the Signal Level and SNR

2.2.1 Signal level and SNR for the Holography Test using the Transmitter Source

The radiating horn used on the transmitter is a standard 20 dB rectangular horn from Custom Microwave. The approximate solid angle of the beam from such a horn is

$$\Omega_A = 4\pi/\mathrm{Gain} = 0.1257 sr \quad (1)$$

Since

$$\Omega_A = \frac{\pi r^2}{R^2}, \tag{2}$$

where R is the distance from the transmitter to the receiving antennas, and r is the radius of the illuminated area, at a distance of 250 meters away from the transmitter, the radius of this illuminated circle can be calculated to be

$$r = 50m, \tag{3}$$

which is appropriate for our initial holography measurement at Haystack.

Using the values of the output power from the transmitter of 12 mw, the diameter of the main antenna disk of 6 m, and an aperture efficiency of 80 % (Zhang 1995), the received power by the main antenna feed at the boresight direction is found to be

$$P_{1a} = 0.8 \cdot \frac{\pi \cdot 3^2}{4\pi 250^2} \cdot 12(mw) \cdot 100 = 0.035mw = -15dBm, \tag{4}$$

where we have ignored the small polarization loss.

The horn on the phase-reference receiver has a radius around 1.4 cm. Assuming a coupling efficiency of 0.8 for the reference horn, the ratio of the power received at the main receiver and at the reference receiver is

$$\frac{P_{1a}}{P_{2a}} = \frac{0.8\pi 3^2}{0.8\pi 0.014^2} = 4.6 \cdot 10^4 = 47dB \tag{5}$$

Therefore the power received by the horn of the reference receiver is

$$P_{2a} = -62dBm \tag{6}$$

Assuming a DSB system temperature of 2400 K (Appendix), the noise power in a 100 kHz bandwidth is found to be

$$W_n = kTsysBW = 1.38 \cdot 10^{-23} \cdot 2400 \cdot 1.0 \cdot 10^5 = 3.4 \cdot 10^{-15} w = 3.4 \cdot 10^{-12} mw. \quad (7)$$

Therefore the signal-to-noise ratio for the main receiver path is

$$\frac{S_1}{N}_{pre-detection} = \frac{P_{1a}}{4W_n} = 2.5 \cdot 10^9 = 94dB, \tag{8}$$

where the factor of 4 in the denominator takes into account of the fact that both the first and and the second mixer are double-side-band mixers.

The signal-to-noise ratio for the reference receiver path is

$$\frac{S_2}{N}_{pre-detection} = 47dB. \tag{9}$$

The above signal-to-noise ratios are the values driving the vector voltmeter. To calculate the post-detection signal-to-noise, we note that the vector voltmeter has an equivalent bandwidth of $1/t$ for the CW signal, where t is the integration time. The noise power for 0.05 sec of integration is therefore (converted to the input of the receivers)

$$N = k(4T_{sys}(DSB))BW \cdot \sqrt{\frac{1}{t \cdot BW}} = 0.6 \cdot 10^{-18} W = -152dBm \tag{10}$$

The signal levels, on the other hand, are given by (4) and (6). Therefore the peak signal-to-noise at the boresight direction is

$$\frac{S}{N}_{post\ detection} \approx \frac{\sqrt{P_{1a} P_{2a}}}{N} = 108dB, \tag{11}$$

2.2.2 Signal Level and SNR during the Astronomical Observations

For an SiO maser of 1000 Jy in a 100 kHz band, the signal level arriving at the receiver input is (taking into account the polarization loss)

$$S_{maser} = \frac{1}{2} Flux\ Density \times Area \times Efficiency \times BW \approx 1.1 \cdot 10^{-14} mW = -140 dBm. \tag{12}$$

For a planet of 500 Jy, the received signal in a bandwidth of 1 GHz is

$$S_{planet} = 5.6 \cdot 10^{-11} mW = -102 dBm, \tag{13}$$

For an SiO maser of 1000 Jy, and for 2 minutes of integration and 100 kHz bandwidth

$$\begin{aligned} \frac{S}{N} &= \frac{Flux \cdot Area \cdot Efficiency}{2 \cdot 2 \cdot 2 k_B T_{sys}(DSB)} \sqrt{BW \cdot t} \\ &\approx 5dB, \end{aligned} \tag{14}$$

where of the three factors of 2 in the denominator, the first two are due to the two DSB mixers, and the third is due to the polarization loss.

The SNR for a planet of 500 Jy in a 1 GHz bandwidth can be calculated to be (assuming 30 second integration)

$$\begin{aligned} \frac{S}{N} &= \frac{Flux \cdot Area \cdot Efficiency}{2 \cdot 2 k T_{sys}} \sqrt{BW \cdot t} \\ &\approx 22dB \end{aligned} \tag{15}$$

where we have only two factors of two in the denominator because here we do not use the second mixer.

2.3 Beacon Transmitter

The 92.4 GHz terrestrial source which illuminates both the main receiver and phase-reference receiver is a phase-locked Gunn Diode oscillator. The varactor-tuned ZAX Gunn oscillator is locked to the sixtieth harmonic of a high-stability, oven-controlled crystal oscillator at 96.34 MHz. The phase-lock loop IF reference signal is provided by a second oven-controlled oscillator operating at 84.96 MHz.

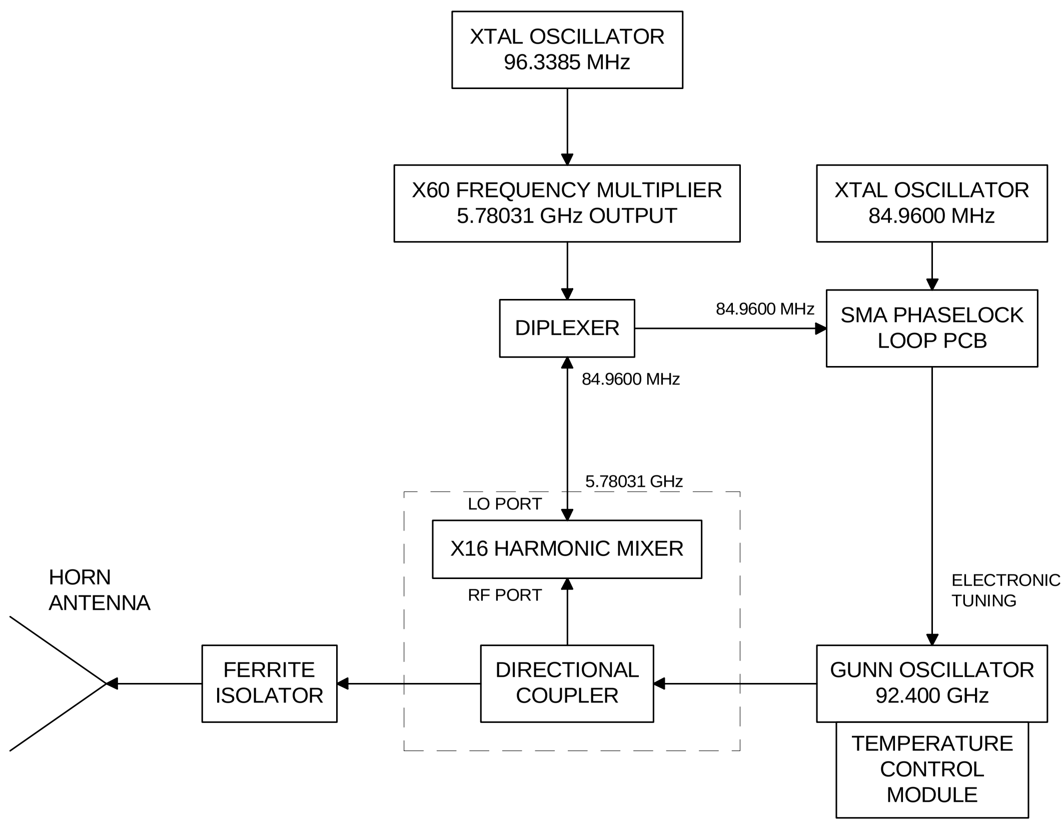

Figure 2: Holography beacon transmitter

Figure 2 is a simplified block diagram of the Beacon Transmitter. A very clean and stable reference signal is generated by the temperature-controlled Piezo Crystal 96.3385 MHz quartz oscillator. The oscillator output is multiplied to 5.78031 GHz by a MITEQ LP-series phase-locked frequency multiplier which, in turn, drives the Pacific Millimeter harmonic mixer through a ferrite isolator and a diplexer. The RF port of the two-port harmonic mixer is driven at 92.400 GHz, through a 10 dB coupler, from the output of the varactor-tuned ZAX Gunn oscillator. Since the 16th harmonic of 5.78031 MHz is 92.48496 GHz, an IF signal at 84.96 MHz is generated at the local oscillator port and routed to the SMA phase-lock loop PCB through the Pacific Millimeter diplexer. In-phase and Quadrature signals, referenced to the 84.96 MHz quartz oscillator signal, are generated on the PCB and used to automatically phase-lock the Gunn oscillator to the reference signals.

The Gunn oscillator output is fed to a horn antenna through a second waveguide ferrite isolator; about 12 mW power is available at the output of the isolator. Auxiliary circuitry incorporated into the Beacon Transmitter provides automatic phase-lock acquisition and reacquisition, temperature control of the Gunn oscillator, remote control of the Gunn oscillator tuning, and temperature and phase-lock status telemetry.

As described above, the Beacon Transmitter is straightforward application of standard phase-lock technology to the 90 GHz band. However, the physical environment is unusually hostile, and a number of special measures were taken to cope with the thermal and electromagnetic compatibility problems. The Beacon Transmitter is mounted near the top of a 80m tower which forms part of an active HF ionospheric sounding system. The HF transmitter periodically sweeps over the entire HF band at radiated power levels of up to 25 kW.

Since the Beacon Transmitter is fully exposed to New England weather in all seasons, particular care was taken with the thermal design of the enclosure. The thermal considerations are complicated by the electromagnetic radiation environment, which precludes the use of air vents, and further complicated by the inaccessible location of the beacon which makes it impractical to incorporate mechanical devices such as fans or blowers. The final design combines passive sun screens, conductive transfer to the cast aluminum housing and active thermal control of the two crystal oscillators and the Gunn oscillator to produce a device which operates effectively over the temperature range -25 to +40 degrees C. The Beacon Transmitter was cycled through the temperature range in a laboratory thermal test chamber and proved capable of automatically acquiring lock after soaking at the temperature extremes, as well as retaining lock over the entire range.

The EMI problem was attacked by housing the Beacon Transmitter in a completely sealed, cast aluminum enclosure. A conductive O-ring around the periphery of the cover plate provides a watertight RF seal. All power, control and telemetry leads enter the EMI-protected volume through multi-section RF filters. The most sensitive section of the transmitter circuitry is the remote Gunn oscillator tuning control; any noise on this line directly modulates the oscillator frequency. To minimize the possibility of EMI contamination on this line, the oscillator tuning adjustment is performed by a potentiometer inside the shielded volume. The potentiometer is rotated by a small DC motor, mounted outside of the shielded volume, which is controlled from the ground. The only deliberate penetration of the housing is the W-Band waveguide which feeds the horn antenna.

2.4 Holography Main Receiver, Phase Reference Receiver and the Back-End

The main receiver operates in the RF frequency range of 85-93 GHz. It serves as both the holography receiver and the system test receiver at the Haystack site. It will be mounted inside the antenna receiver cabin, at a location close to the Cassegrain focus of the antenna (Zhang 1995, section 4). Since the main holography receiver is in the nominal optical path, one of the requirement for its mechanical design is its easy removal during regular observations with high-frequency receivers, and its easy re-attachment during the holography experiment without the need to re-align the optics. Both of these are made possible by the use of the Thorlabs optical kinematic mount. Furthermore, since the only possible location for the main receiver on the optical axis is a very tight space between the weather window in front and mirror No. 4 behind, there is a stringent requirement of compactness on its mechanical design.

In Figure 3, a simplified block diagram of the main holography receiver is given. In the holography mode (with the terrestrial transmitter), a 92.4 GHz signal is coupled into the scalar feed through the aperture lens. Regarded as in the transmitting mode, the feed/lens combination results in a flat wavefront at the front surface of the lens,

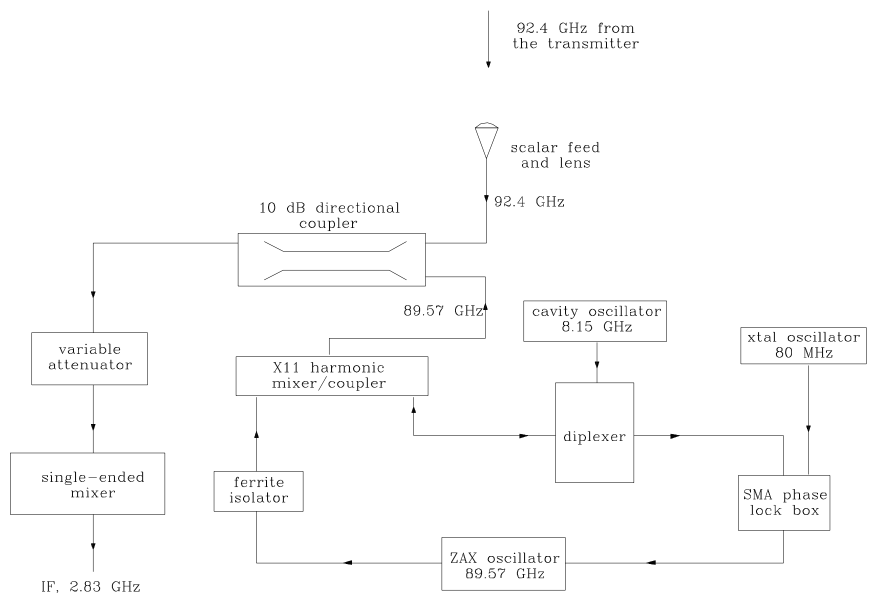

Figure 3: Holography main receiver

and it produces about 11 dB edge taper on the subreflector (Zhang 1995).

The incoming RF signal is combined with the LO signal (at 89.57 GHz) through a Millitech 10 dB directional coupler, which are then fed into a Millitech single-ended mixer to obtain the 2.83 GHz IF signal.

The phase-lock circuitry for the ZAX oscillator is very similar to that for the transmitter, except that the turing voltage range for this particular ZAX oscillator goes from 0 V to about 25 V, so a modification of the regular SMA phase-lock (which has a turing range of 0 - 10 V) had to be made.

The holography phase-reference receiver uses a small scalar feed and a phase corrector lens to provide a constant phase standard as the antenna pivots about its axis. The reference receiver (Figure 4) has a very similar electrical design as the main receiver, except that the single-ended mixer/directional coupler module is replaced by a Millitech balanced mixer. The mechanical design of the phase-reference receiver, however, has its unique set of stringent requirements due to its location inside the small cylindrical-shaped space at the back of the chopping-subreflector control housing. The final design mounts both the receiver and the phase-lock PCB onto the back-cover plate of the housing cylinder, so the whole receiver module can be removed from (or placed onto) the chopper housing as a single piece. It also provides a tight weather seal between the environment and the internal space of the chopper housing, which contains both the receiver and the chopper control circuitry. When the phase-reference receiver is not in place, a dummy plate is used to cover the back of the chopper housing.

The back-end of the holography data acquisition system has already been shown in Figure 1. In the first configuration, the pre-amplified IF signal at 2.83 GHz for each path is further down-converted to 21.4 MHz, using MITEQ DSB mixer. The signal then passes an Mini-Circuit LPF, a 3 dB attenuator pad (not shown), a Network-Sciences 100 kHz BW BPF, before the final detection at the HP vector voltmeter. The two second-LO signals for the MITEQ mixers are generated through a synthesizer at 1239.3 MHz, followed by a Mini-Circuit doubler, an MITEQ amplifier and a Mini-Circuit power splitter.

The second configuration (SiO maser observation) uses only the main receiver path, and a total power detector is connected to the output of the 100 kHz BPF.

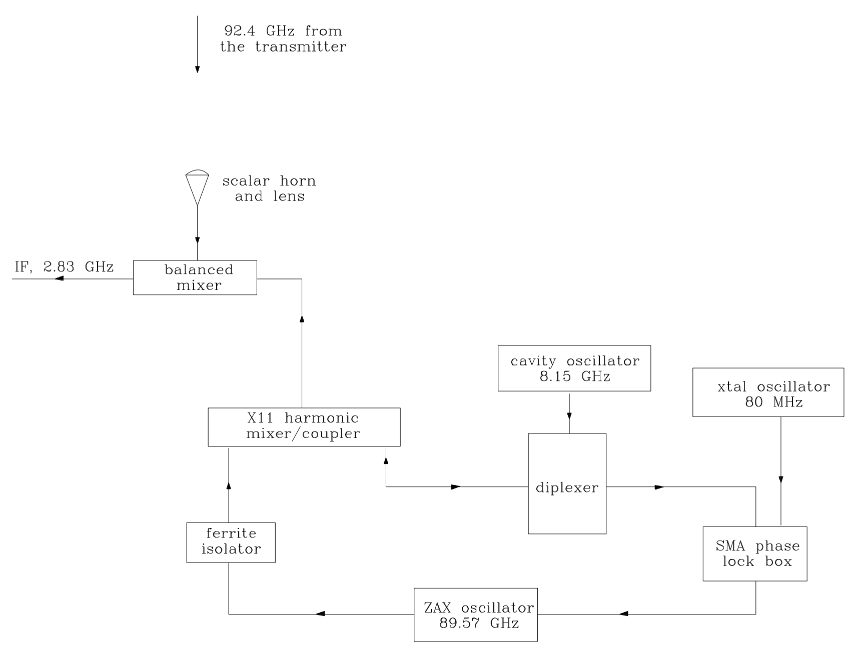

Figure 4: Holography phase-reference receiver

The third configuration (planet observation) uses a 2-3 GHz BPF directly following the first receiver output, and total power detection is made after pre-amplification.

3 Data Acquisition Software

3.1 General Strategy for Data Acquisition

The beam pattern of the antenna is measured on a square grid of N by N in size (normally N = 128), by rotating the antenna to different azimuth and elevation angles, with the transmitter fixed in space. This results in a beam map which is effectively distributed on a spherical surface, with the center of the sphere being the pivoting point of the antenna (= the intersection of the azimuth and elevation axes). This is the desired distribution to result in a Fourier transform relation between the measured beam pattern and the aperture field (Zhang 1995, section 6). The samples on the grid are uniformly distributed in angles.

The ordering of data in the beam map conforms to the convention used in the data analysis software. First of all, since the data analysis software requires that N be a power of two, with the center of the map at (N/2 +1, N/2+1) on the beam map (as well as on the aperture map), we use the same convention during the data acquisition process. Furthermore, since the analysis software expects that the data being taken as a series of row scans in the order of increasing azimuth for each (increasing) elevation, during the data acquisition process we steer the antenna in the reverse order, i.e. starting from the highest elevation and largest azimuth point, and scan in the order of decreasing azimuth for each (decreasing) elevation, so as to obtain a beam map with the data arranged in the correct order.

The normal data rate during the data acquisition is 10 points per second (for the averaged data), so a 128 by 128 map should take on the order of half an hour to complete. There is of course overhead time for steering the antenna to the beginning of each row and to the boresight periodically (usually before each row scan) to acquire calibration values. Taking into account the overhead time a 128 by 128 map should still be able to be done in less than an hour. This ensures that the changes in atmosphere condition during each map measurement is minimal.

The raw data rate is usually 10 times as high as the averaged data rate, and the data is taken "on-the-fly" during each row scan. The central 50% of the raw data in each map cell is averaged, and saved as the averaged data for that cell.

The actual data acquisition software is distributed on three different types of computers: (1) On the gateway computer there is a user interface implemented with X-window routines. It receives the measurement parameters and the general control commands from the user, and it also displays the measured data in real time. (2) On the antenna computer there are routines which receive the user inputs from the X-program, translate them into the actual motion procedures to command the PMAC to steer the antenna, and to record the data. The averaging of the raw data from the PMAC is also done on the antenna computer before sending them back to the X-program for storage and display. (3) The low-level PMAC routines receive the control commands from the antenna computer, steer the antenna in the desired fashion and write the data into PMAC's DPRAM, to be read by the routines in the antenna computer and to be sent back to the X-program. In what follows, a detailed description of each of these three levels of programs is given. We will describe here only the main holography data acquisition package. Two auxiliary packages, one for boresight acquisition and the other for determining the instrumental delay, also exist in the general holography directory and have very similar structures as the main holography package.

3.2 The X-Window User Interface

The X-window program provides the user with the ability to control the holography data acquisition process. It also provides a real-time display of the holography data during acquisition.

The control, status, and measurement data I/O between the X-program and the acquisition programs on the antenna computer are performed using reflective memory. The reflective memory consists of a fiber optic link and 256 Kbytes of shared memory between the various SMA computers (nodes). The reflective memory is mapped into VME address space and is common to all nodes. Details of the reflective memory may be found in the SMA memo on "Reflective Memory Use for SMA Communications" by R. Calder & P.Bratko - Feb 1, 1995.

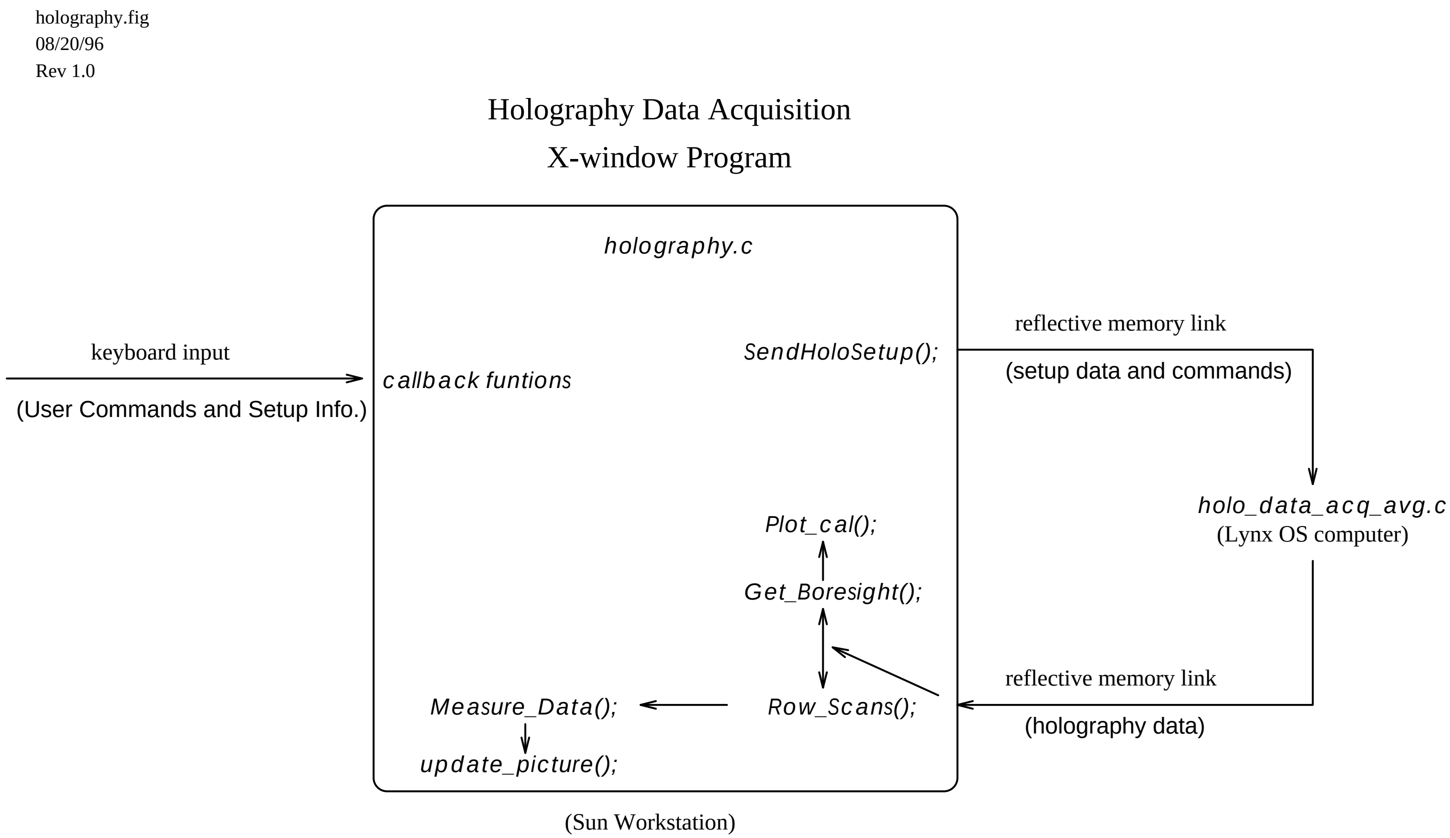

Figure 5: Holography X-Window Program

The internal processing of the X-program including its reflective memory link to the antenna computer is depicted in Figure 5. As with many X-window programs, the user input is fed in through the graphics display window and is acquired by the X-program through the use of X-events and callback functions.

A detailed description of the X-program processing is beyond the scope of this memo. Here are is a brief overview of a typical session:

- The user invokes the program.
- The program initializes itself and updates reflective memory with a default setup.
- The user updates the measurement parameters on the screen if necessary.
- The user 'clicks' on the start button.
- The program reads the setup parameters from the screen, and updates the values in reflective memory.
- The program performs handshake with the acquisition program on the antenna computer to make sure it is running.
- For each row scan, the program sends the start command to the antenna computer, polls the reflective memory for new data or error states, and then reads the data and updates the display OR reads the error response and updates the status window.
- The row scan loop continues till completion.

The user interface is shown in Figure 6. Here is a brief description of the display.

Measurement Parameters Window:

The *Measurement Parameters* section allows the user to configure the setup as desired. A description of the configurable items is as follows:

Pnt Ctr in Az (deg):

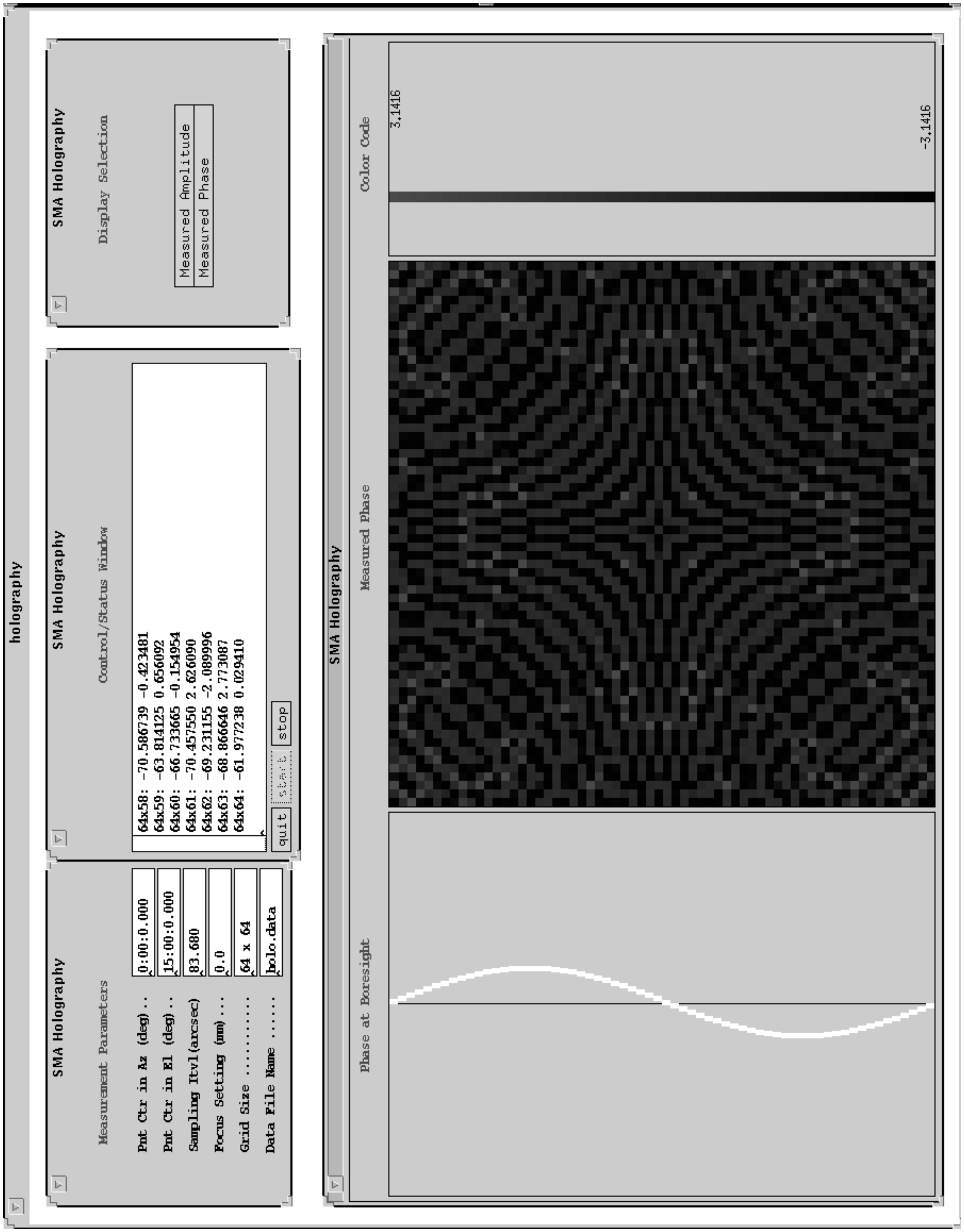

Figure 6: Holography X-window user interface

Azimuth of boresight. Azimuth pointing center value is saved internally in units of milliarcseconds.

Pnt Ctr in El (deg):

Elevation of boresight. Elevation center value is saved internally in units of milliarcseconds.

Sampling Itvl (arcsec):

Sampling Interval - Size of each measurement cell. Note that the grid size is 128 x 128. In this example, 128 cells * 83.68 arcsec results in a scan window of approximately +/- 1.5 degrees. Sampling interval is saved internally in units of milliarcseconds. The default 83.68" sampling interval results in a 8m by 8m aperture map.

Focus Setting (mm):

Subreflector focus position. The internal representation of this field is in units of micrometers.

Grid Size:

This is the number of cells to measure. The first value is for azimuth and the second for elevation. These values must to be a power of 2.

Data File Name:

The holography data will be archived to disk. The field contains the name of the data file. Three data files will be saved: the raw data file and the averaged data file for regular row scans, as well as the boresight calibration data file. All the data files will be saved by and on the antenna computer. The data file name will have two kinds of extensions appended to it. The first kind is an *avg*, *raw* or *bore* extension to indicate the type of data; the second is a date and time stamp. In this example, the resulting data files taken on May 28, 1995 at 10:30 AM would be named:

holo.data.avg.950528_1030 holo.data.raw.950528_1030

Control / Status Window

The Control / Status Window provides buttons and a text display area. The display area echos measured data, status, and error information. The buttons start or stop the holography data acquisition or terminate the program. Quitting the program also causes the other programs (PMAC and antenna computer) to terminate. Termination will proceed in an orderly manner.

Display Selection Window

In the *Measured Data* display window (which will be described below), there are two overlaid windows - one for amplitude data, the other for the phase data - that can be cycled by the buttons in the *Display Selection* window . The corresponding boresight information and the colorcode for the measured data will be simultaneously selected.

Measured Data Window

As stated above, this window is actually two overlaid windows. Each window consists of three sections as follows:

- Amplitude (Phase) at Boresight: This is the boresight data corresponding to each azimuth scan. Boresight data is taken at the start of each azimuth scan, and after the last scan.
- Measured Amplitude (Phase): This section represents the measured data on the (user specified) grid. The data is color-coded to indicate relative magnitude or phase.
- Color Code: This is the color code for the measured data.

3.3 The Data Acquisition/Averaging Software on the Antenna Computer

The data acquisition and averaging software consists of four programs, all running on the antenna computer. The first program, holo_data_acq_avg.c, waits for a start command from the user interface and then performs a regular row scan, as well as average the data. The remaining three programs, holo_write_raw_data.c, holo_write_avg_data.c, holo_write_bore_data.c, are the children programs created by the holo_data_acq_avg.c, which write the data into the respective data files asynchronously as the data are taken and averaged, and relay the averaged as well as the boresight data to the X-program using reflective memory. The primary flow of data between the two types of programs is through LynxOS shared memory segments. Here is a conceptual flow of the processing:

Since the holo_data_acq_avg.c program is doing the majority of the processing, an elaboration of its functionality is given below.

- When invoked, the program allocates LynxOS shared memory segments which it uses for processing the holography data.
- The program waits for a start command from the reflective memory (originates at the X-program).
- The setup data is read from the reflective memory.
- The vector voltmeter is initialized (using the GPIB) and the focus is set.
- The program now enters a loop which will first measure calibration data at the boresight and then scan in azimuth for the measurement data. The loop iterates over the elevation range. Here are the loop details:
  - Command the PMAC to the boresight position.
  - Read the boresight data values from the PMAC DPRAM.
  - Command the PMAC to the starting azimuth position for the current elevation (elevation is the looping variable).
  - Command the PMAC to perform a LINEAR move to the end azimuth position.

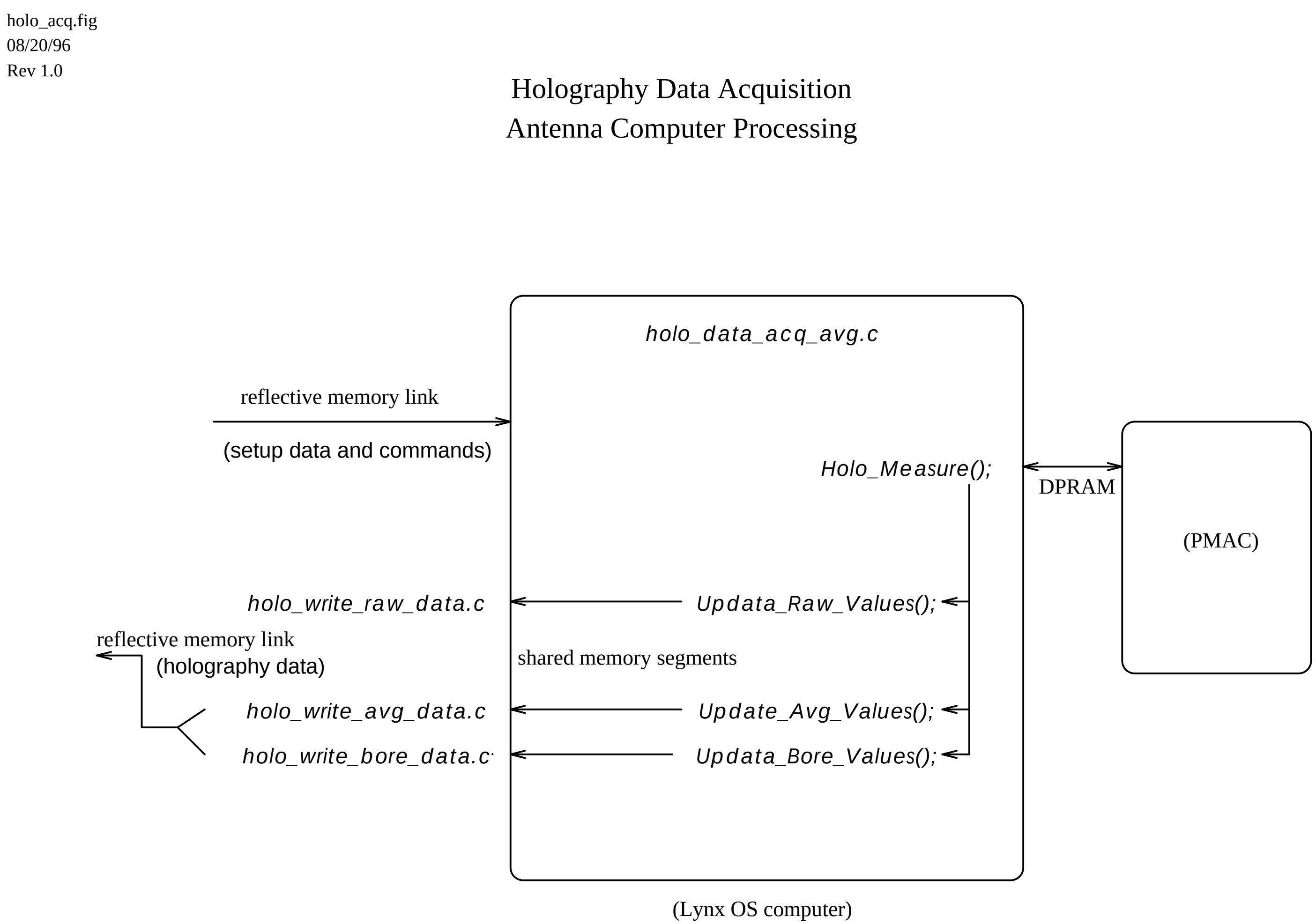

Figure 7: Holography Data Acquisition Programs on the Antenna Computer

  - While the PMAC is performing the LINEAR move, read the encoder data for the azimuth and elevation, amplitude data, and phase data at an approximate 100 Hz rate. Save this data in the data buffer.

- Average data for the current row scan.
- Close the data file.

The averaging algorithm reads the data from the raw data buffer, averages it, and writes the averaged value to the average data buffer. The middle 50% of the data for each cell is averaged and saved.

3.4 Software for the PMAC

The PMAC performs its services for holography using motion programs and "plc" programs, which move the antenna to the boresight and take the data, or move the antenna along the azimuth (using a LINEAR command) during a row scan. The PMAC communicates with the host program (holo_data_acq_avg.c) through the use of dual-ported RAM. This memory is mapped into VME address space. A simplified diagram illustrating the functioning and communications of the programs reside on the PMAC is give in Figure 8.

The PMAC measures four pieces of data at each data location, they are:

#1: azimuth position
#2: elevation position
#3: amplitude data from the vector voltmeter
#4: phase data from the vector voltmeter

The data are saved by the PMAC into user defined DPRAM locations and a "new data" flag will be set to indicate to the antenna computer that there is data to read, which is then cleared by the antenna computer after the reading is completed.

Several DPRAM locations are reserved for setup and synchronization between the host and the PMAC. These locations, as with all VME mapped memory locations in the entire SMA software realm, are identified in various C language include files.

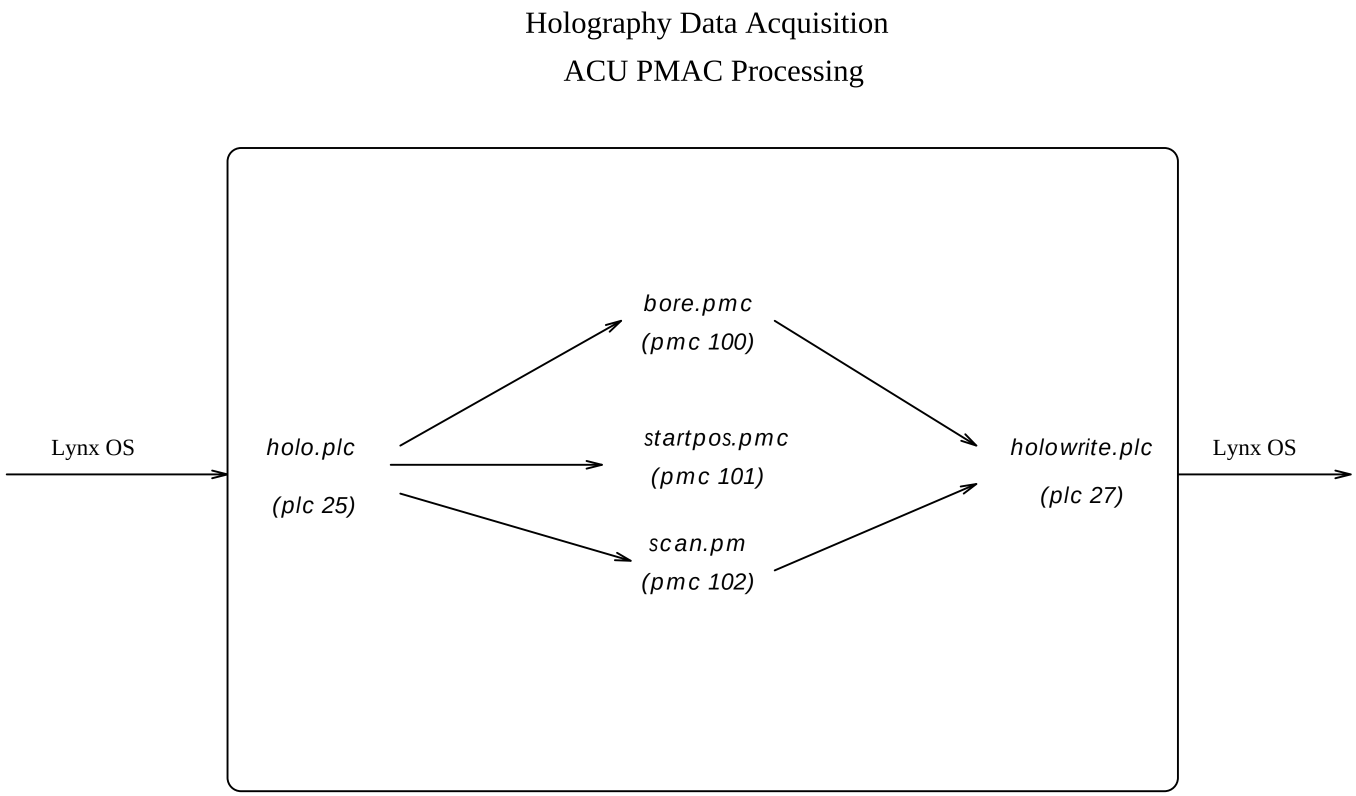

Figure 8: Holography Data Acquisition Programs on the PMAC

4 Data Analysis Software

The data analysis software package, HOLIS, is written in FORTRAN 77. It currently implements the phase-coherent aperture-field-recovery scheme. The implementation of the phase-retrieval algorithms will be added to the package soon.

The HOLIS routines reside mainly in three separate directories: *preprocessing*, *inversion*, and *panelfit*, which correspond to the three stages for the processing of the measured data. The tasks performed by the routines in these three directories are described in details in the following.

4.1 Preprocessing

This is the first stage in data processing. The input data, in the form of two files containing the amplitude and phase distributions of the beam pattern, respectively, are assumed to be taken on a grid N by N in size, in the order of increasing azimuth for every (increasing) elevation. The preliminary calibration of the measured data to remove systematic drifts is assumed to have been done before this stage on the gateway computer.

The routines in this subdirectory perform mainly three tasks:

1. Determining the phase-reference plane (which is usually chosen to be half-way into the depth of the main reflector to minimize diffraction effect) by performing the correction to the measured phase described in Zhang (1995), section 5.

2. The choice of increasing the resolution on the aperture plane by patching zeros in the area outside the measurement grid, to create effectively a larger-sized measurement grid for both the amplitude and phase files of the beam pattern.

3. The choice of weighting the far-field amplitude by a Gaussian to reduce the effect of aliasing.

Both the procedure of item 2 and 3 are expected to be necessary only when we do holography on a celestial source, where a smaller map is taken.

4.2 Obtaining the Aperture Field

In the phase-coherent holography algorithm, the aperture field is obtained from the measured far-field pattern, usually obtained from the output in the *preprocessing* directory, through a direct Fourier transform (a forward FT in our convention). One intricacy involved here is the issue of original shift, since normally an FFT routine will put the low-frequency components on the edges of the frequency domain. For the actual measured far-field pattern, which has a peak in the central region of the map, it turns out we need to do an origin shift both before and after the FFT, in order to recover the correct aperture distribution, i.e. that which has a platform near the central region of the map. If the far-field pattern used is from an (inverse) FFT followed by an origin shift, as is the case for our example below, which also peaks near the center, we only need to do an origin shift before the FFT to recover the correct aperture distribution in this second case, with no need to do an origin shift after the FFT.

The recovered aperture distribution is then masked for the subreflector blockage (possibly also the feedleg blockage in the future) and for the area outside the edge of the antenna dish. The aperture phase is adjusted to correct for the near-field effect (Zhang 1995, section 6). At this point we have obtained an aperture phase distribution ready to be fitted for large-scale errors.

In the current implementation of HOLIS we fit for 5 kinds of large-scale errors: (1). A constant term. (2). A linear gradient term in the x direction. (3). A linear gradient term in the y direction. (4). A defocus function (Ruze 1969). (5) The secondary-mirror diffraction pattern. No second-order terms are fitted since it is easily confused with the diffraction term (Zhang 1995, Appendix II). The surface rms phase errors before and after the large scale fitting are calculated, and a residual phase map is written out to be copied to the *panelfit* directory to calculate the panel movement needed to compensate for the residual error.

In the following, we present an example demonstrating the use of the routines in this directory to calculate the aperture distribution and to fit large-scale errors.

We use the software package MATLAB to generate an aperture distribution which has a constant amplitude across the aperture except for the subreflector blockage, and which has a phase distribution corresponding to 0.32445 mm (= 0.1 λ at 92.4 GHz) defocus. The far-field amplitude and phase are obtained from the (inverse) FFT of the above aperture distribution.

We now input this far-field data file to our HOLIS package, and calculate the aperture distribution and fit for the large scale errors. Here is a summary of what the program returns:

Number of the large scale fitting parameter = 5
rms before the phasefit = 9.3672989816612D-02 radian
coef(1)= 2.1423660780575D-09 ! constant offset
coef(2)= -8.8478583605566D-11 ! tilt in x direction
coef(3)= -1.1504121043566D-10 ! tilt in y direction
coef(4)= 0.32445021666746 ! defocus in mm
coef(5)= 9.6415969155128D-09 ! diffraction term
chisq= 7.1776506986915D-12
rms after the phasefit = 3.1630453564464D-08 radian

We see that the program correctly calculated the aperture field, and the fitting routines attribute most of the phase distribution in the defocus term, and gives an estimated amount of defocus which is almost exactly equal to what we started with. Very little is attributed to the rest few large-scale error terms.

4.3 Panel Fitting

From the recovered aperture phase map $Ph(x, y)$, where x, y are the cartesian coordinates on the aperture plane, a surface error map can be derived (Zhang 1995, section 1). Specifically, the error map $\epsilon(x, y)$ is related to the phase map $Ph(x, y)$ through

$$\epsilon(x, y) = \frac{\lambda}{4\pi}(1 + \frac{x^2 + y^2}{4F^2})^{1/2} \cdot Ph(x, y) \quad (16)$$

where F is the primary focal length of the antenna, and where $\epsilon > 0$ means that the panel is moved outward from the correct location.

The actual panel screw movement needed to compensate for the aperture error distribution is calculated using the least-square fitting approach. The motions for all

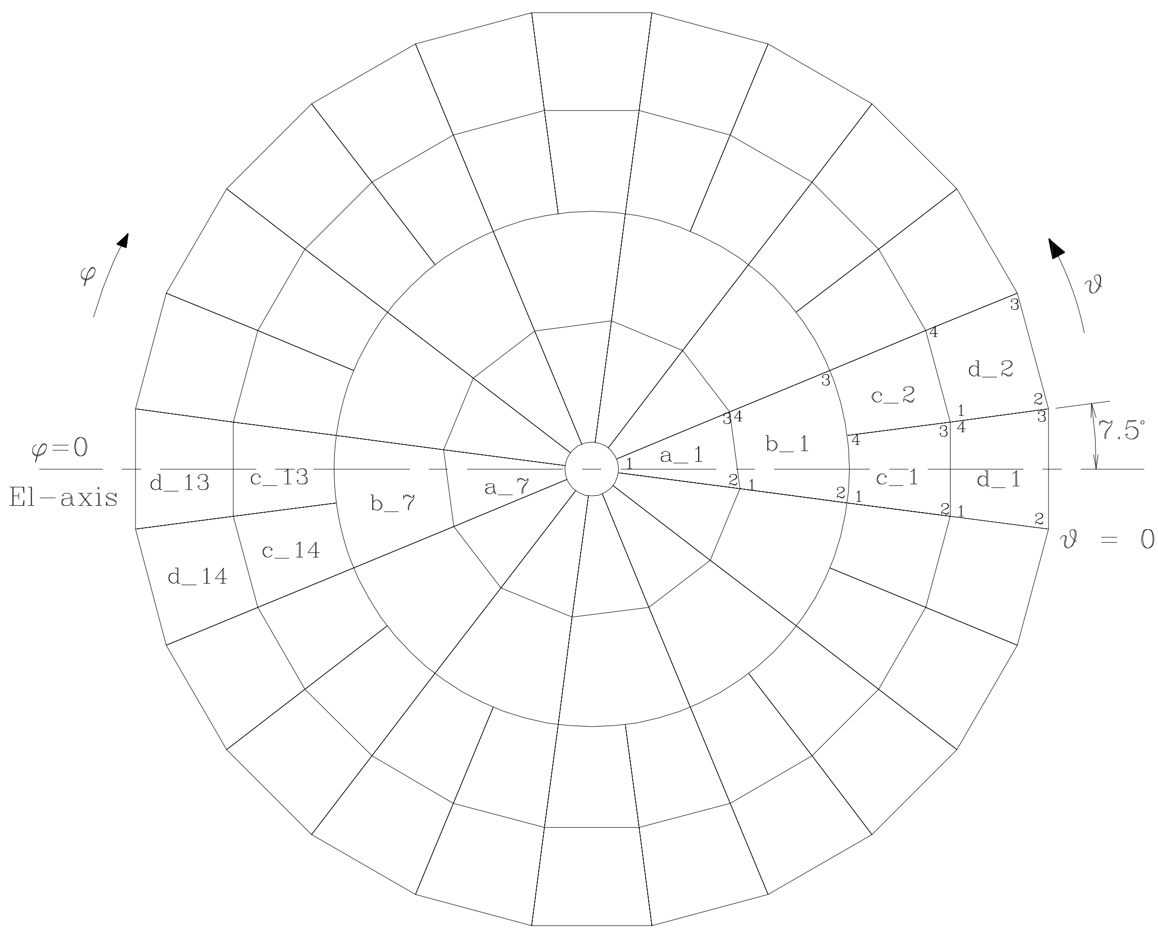

Figure 9: Frontview of the SMA antenna dish

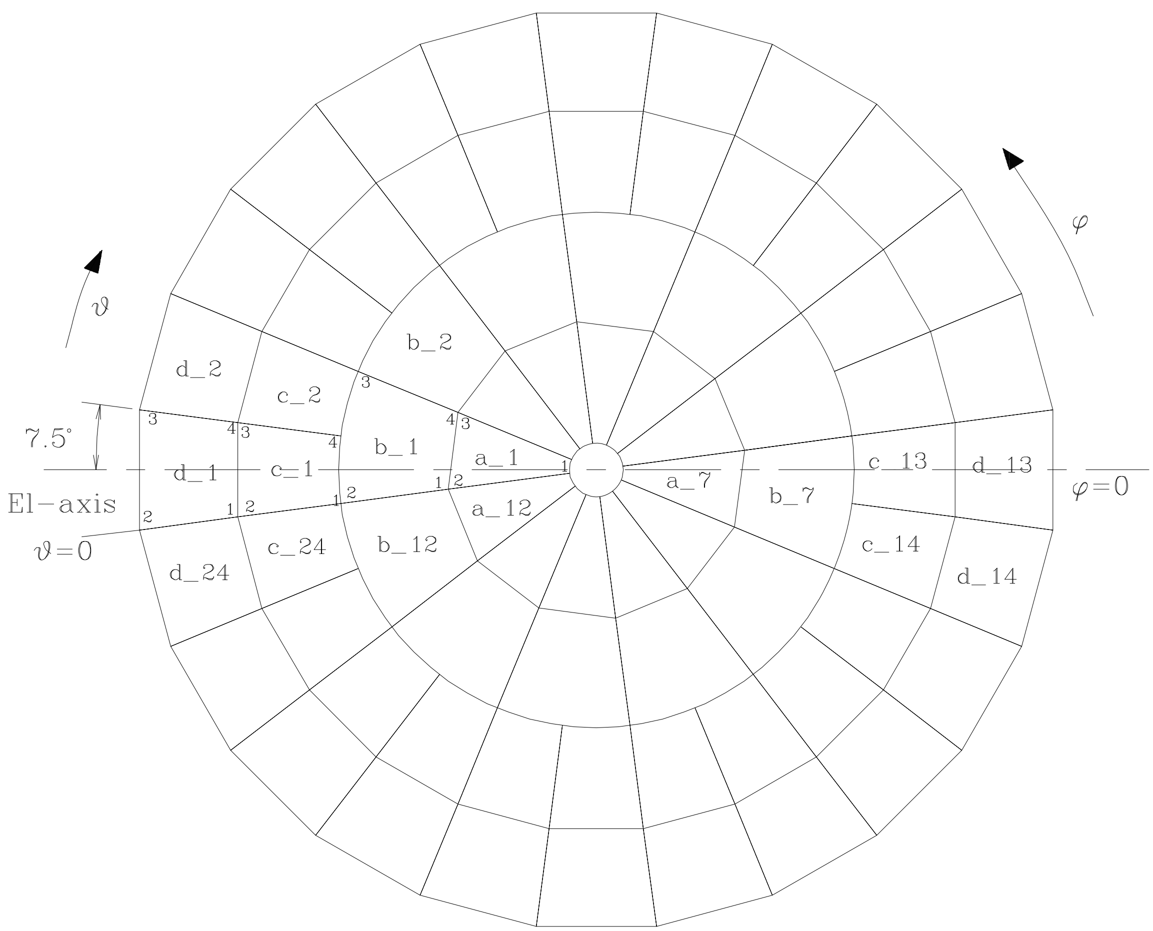

Figure 10: Backview of the SMA antenna dish

four screws (or all three screws for the first row) of a panel are calculated simultaneously using all the data points which fall within the range of the panel, with possible boundary masks.

In Figures 9 and 10, the front and back view of the SMA antenna panels, together with the naming convention for panels and for the screws on each panels are given. Note that there is a 7.5^o rotation in the arrangement of the panels, so the symmetry with respect to the elevation axis is lost.

The Fourier transform and the panel fitting programs refer to an aperture phase distribution which is effectively the backview of the antenna (Figure 10), whereas the actual setting of the screws is done from the front of the antenna dish. In order to minimize confusion our naming convention established an exact correspondance between the front and the back views. Specifically,

- In both the front and back views, the first row of panels is the innermost row, numbered a_1 through a_12, with the first panel starting from left (for front view) or right (for back view) side of the dish center, and its first radial edge 7.5^o below the elevation axis. The numbering then run counter-clockwise (for front view) or clockwise (for back view). Similarly for panels b_1 through b_12, c_1 through c_24 and d_1 through d_24. The first edge of the first panel in each row corresponds also to $\theta = 0$ in the panel fitting programs.

- The first row of the main reflector panels have three screws, and the rest of the panels have four screws. The numbering of the screws is such that for each panel, the first screw is the one which has the smallest r and θ value, and the second, third and fourth screws run counter-clockwise (for front view) and clockwise (for back view) from the first screw. Note that the angle θ also runs in different directions for the front and back views.

- In the panel fitting programs, a second angle, ϕ, is also used. $\phi = 0$ corresponds to the left side of the elevation axis and runs clockwise for the front view, and it corresponds to the right side of the elevation axis and runs counter-clockwise for the back view. The relation between the θ and ϕ coordinates are: $\phi = 180^o - \theta + 7.5^o$.

Using the above convention, therefore, the movement calculated for screw #1 on panel a_1, say, from the backview of the antenna structure can be directly used to set the screw #1 in panel a_1 from the front without the need for further conversion.

The general procedure for the panel fitting is as follows:

1. Before invoking the main program package *panelfit.com*, first we need to generate the coordinates of the nodes and screw positions for every panel, by running the program *nodes.f*. The coordinates are saved in two tables, *nodes.table* and *screws.table*. The following items then further describe the panel fitting procedure in the main program.

2. Pick a panel (the usual order for doing panel fitting is from a_1 through a_12, ... d_1 through d_24), read out its nodal positions from *nodes.table*, and its screw locations from *screws.table*.

3. Using the nodal coordinates information, calculate the radial and angular limits of the panel, which are then used by the searching program to find all the data points which fall within the range of the panel.

4. Using all the data points for the relevant panel, do a least square fit to calculate the coefficients of the error function (a general second order function).

5. Using the thus-determined error function, calculate the value of the error at the location of the screws. The negative of this value gives the motion of the screw needed to compensate for the error.

6. write out the screw motion into a table, for all the screws on every panel.

Note that since many panels of the SMA reflector have four screws, and since the panels themselves are not perfectly rigid, the general first order function $\epsilon(x,y) = ax + by + c$ is no longer adequate for determining the four degrees-of-freedom screw motions. We therefore choose to use a general second order function $\epsilon(x,y) = ax + by + c + dxy + ex^2 + fy^2$, which has six unknown coefficients. For 128 by 128 map we make, an average panel has from 60 to 115 data points fall within its range, even after masking out a certain amount of data near the edges of panels, which are more than enough to fit the six coefficients. After the error function is thus determined, we can calculate the corresponding error at ($\mathrm{x_{screw}}$, $\mathrm{y_{screw}}$) locations. Since there are at

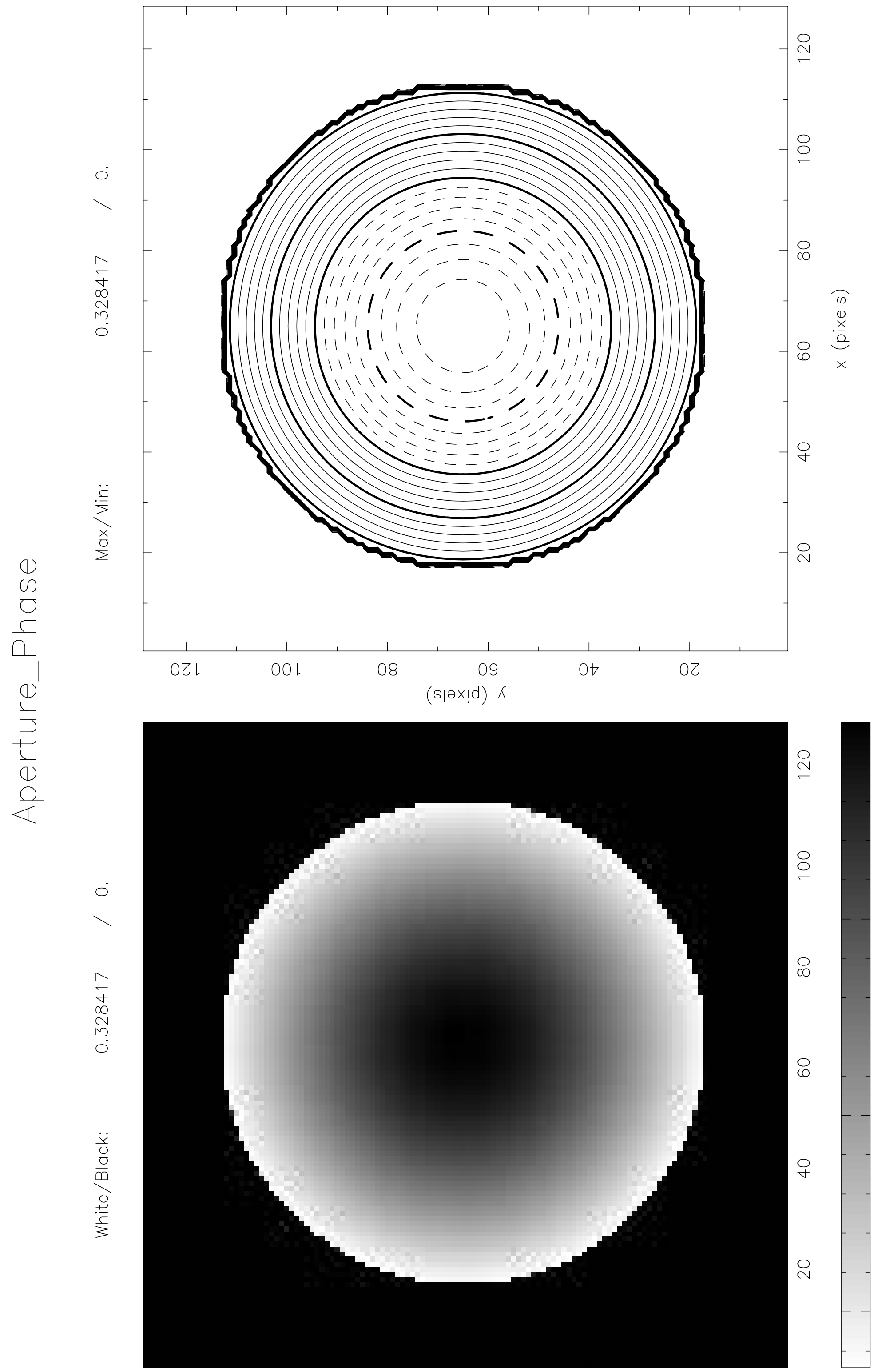

Figure 11: An aperture phase distribution (in radians) corresponds to 0.1 λ subreflector movement

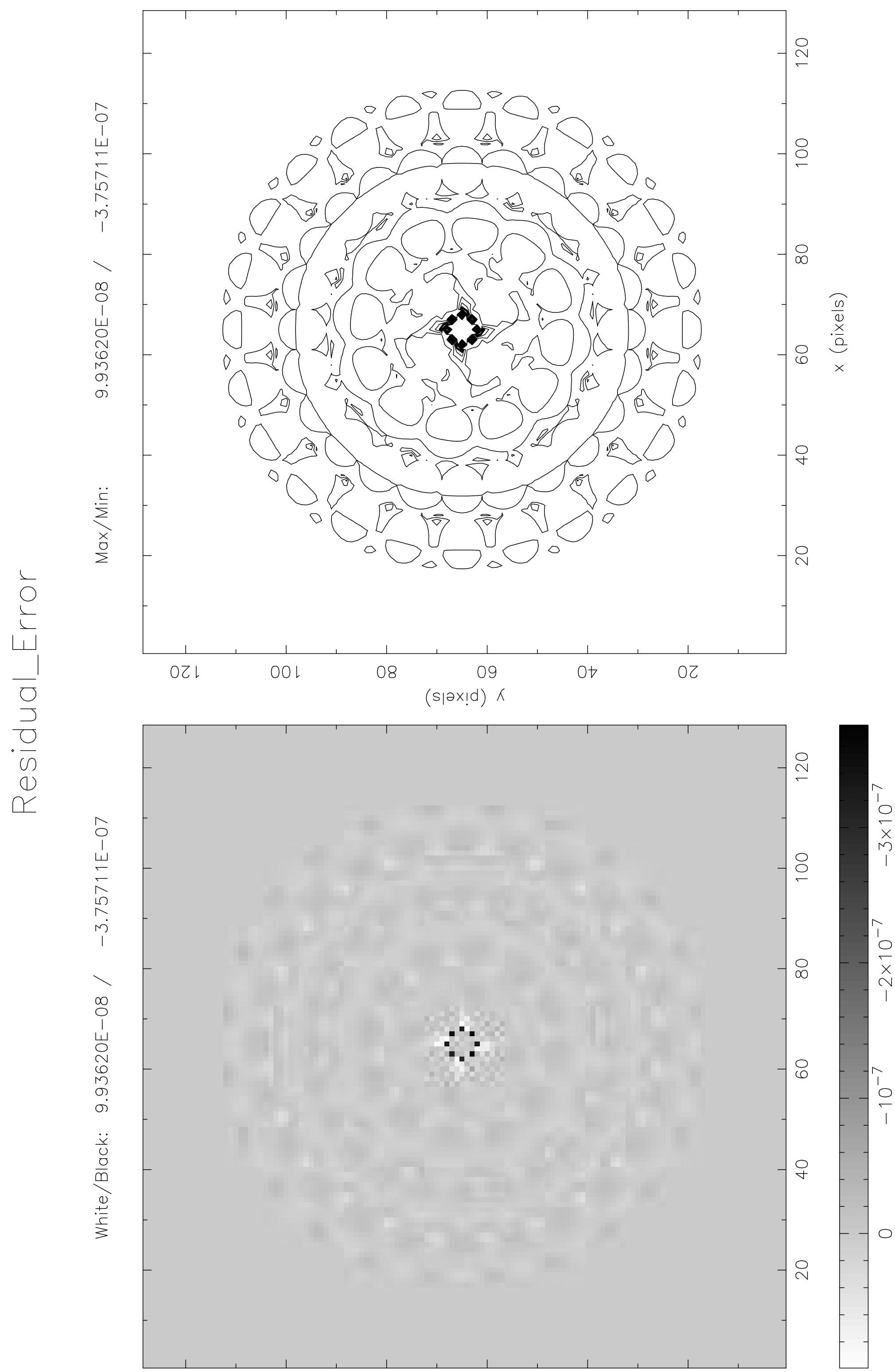

Figure 12: Residual surface error (in meters) after fitting and adjusting the panels

most four screws on each panel, only four independent degrees-of-freedom are actually utilized even with the six fitted coefficients.

In the following, we give an example of the panel-fitting process. We start with an initial aperture phase distribution, shown in Figure 11, which corresponds to 0.1 λ defocus. We try to compensate this aperture phase by fitting and adjusting each individual panels, and then calculate the residual error distribution. Figure 12 shows the result of the residual error map after running the phase map in Figure 11 through our panel-fitting pragram. It is seen that the maximum residual phase error is at the sub-μm level, and even this residual error is mostly due to that the defocus error is of a different functional form than that due to the movement of the panels. The surface rms drops from 34.8 micron before the panel-fitting to $6 \cdot 10^{-3}$ micron after the panel-fitting, which is a factor of 5000 reduction. We therefore conclude that the panel-fitting package is working properly.

5 Summary

The first stage of the holography test for the panel alignment of the SMA antennas will be carried out at the Haystack site, Westford, MA, using a terrestrial transmitter and two 90 GHz receivers, with one of the receivers serving as the phase-reference. The data is taken on-the-fly, with a data rate about 10 points per second, and a total grid size of 128 by 128 points. The algorithm used for calculating the aperture field distribution from the measured beam pattern is that of the phase-coherent Fourier transform method. The initial test is planned for the fall of 1995. For the next stage we will look into the issue of doing holography with a planet source; the implementation of the phase-retrieval holography algorithms (since the current vector-voltmeter setup cannot measure the continuum radiation of a celestial source, so we need to switch to total power measurement when checking the effect of dish deformation versus elevation using celestial sources). Eventually, we expect that the holography measurement will be done using the high-frequency receivers with a correlator back-end at the Mauna Kea site.

Appendix Calculation of the Receiver Noise Temperature and System Temperature

The noise of a component is specified as the noise power at its input that would produce the same output noise power if this component is an idealized noiseless component.

Assuming that the signal power incident onto the front surface of the feed lens is S_{in}. Then the signal at the output of the IF amplifier S_{out} is

$$S_{out} = S_{in} \cdot G_w \cdot G_f \cdot G_m \cdot G_{IF} \equiv S_{in} \cdot G, \tag{17}$$

where:

- G_w = Gain of the lens (window) ≈ 1.
- G_f = Gain of the feedhorn and waveguide ≈ 1.
- G_m = Gain of the mixer.
- G_{IF} = Gain of the IF amplifier.

The noise output after the IF amplifier is

$$\begin{aligned} N_{out} = k_B B\{[(1 - G_w^{abs})T_{phy}(lens)]G_f G_m G_{IF} \\ [(1 - G_f^{abs})T_{phy}(feed)]G_m G_{IF} \\ +T_m G_m G_{IF}\} \\ +T_{IF} G_{IF}, \end{aligned} \tag{18}$$

where k_B is Boltzmann's constant, B is the bandwidth of the receiving system, T_{phy} is the physical temperature of a component, and G^{abs} is the absorption gain of a component.

Therefore,

$$
\begin{aligned}
T_{rcvr} &= \frac{N_{out}}{k_B B G}, \\
&= \frac{(1-G_w^{abs})}{G_w} T_{phy}(lens) \\
&+ \frac{(1-G_f^{abs})}{G_w G_f} T_{phy}(feed) \\
&+ \frac{T_m}{G_w G_f} \\
&+ \frac{T_{IF}}{G_w G_f G_m},
\end{aligned}
\tag{19}
$$

where the noise contribution from after the first IF amplifier has been ignored.

Since the absorption losses of the lens and the horn are small compared to the contribution of the other two terms, we get

$$
T_{rcvr} \approx \frac{T_m}{G_w G_f} + \frac{T_{IF}}{G_w G_f G_m}. \tag{20}
$$

Now we know that the SSB noise figure NF of the mixer is around 7 dB for the single-ended mixer used on the main receiver (it is about 8 dB for the double-balanced mixer used on the reference receiver). Since

$$
NF(SSB) = 10 \log F(SSB) = 7(dB), \tag{21}
$$

therefore the noise factor F is

$$
F(SSB) = 5. \tag{22}
$$

Therefore

$$
T_m(SSB) = (F-1) \cdot T_0 = (5-1) \cdot 290 = 1160, \tag{23}
$$

and

$$T_m(DSB) = \frac{1}{2}T_m(SSB) \approx 580K. \tag{24}$$

For the Millitech mixer we used, the conversion loss is approximately equal to the noise figure, i.e. $L_m = \frac{1}{G_m} \approx F$, therefore

$$G_m(SSB) = \frac{1}{\frac{T_m(SSB)}{T_0} + 1} = 0.2, \tag{25}$$

and

$$G_m(DSB) = 2G_m(SSB) = 0.4. \tag{26}$$

We also have $NF_{IF} = 1.8dB$, therefore

$$F_{IF} = 1.5, \tag{27}$$

and therefore

$$T_{IF} = 145K \tag{28}$$

and

$$\frac{T_{IF}}{G_w G_f G_m} = 362.5K \tag{29}$$

Therefore

$$T_{rcvr}(DSB) \approx 942.5K. \tag{30}$$

During the actual measurement, we have measured a DSB receive noise temperature on the main receiver of about 1300 K at 92.4 GHz RF, and about 1900 K at 86 GHz RF (since at the corresponding LO frequency of the 86 GHz RF, the ZAX Gunn oscillator puts out less power, so the LO is not optimize at 86 GHz RF, thus the mixer performs poorer at 86 GHz RF). For the phase reference receiver, we have measured a receiver temperature of about 1500 K at 92.4 GHz RF. The extra noise contributed by the dielectric lens and the wavedguide components are responsible for the difference between the calculated the the measured values.

The system temperature during the actual observing can be calculated to be

$$T_{sys} = (e^{\tau_{atm}} - 1)T_{atm} + e^{\tau_{atm}} T_{rcvr}. \tag{31}$$

Using

$$T_{atm} = 290K, \tag{32}$$

and

$$\tau_{atm} = 0.2 \tag{33}$$

Using the worse case receiver noise temperature of 1900 K, we obtain

$$T_{sys}(DSB) \approx 2400K \qquad (for\ \tau = 0.2). \tag{34}$$

Acknowledgement

We thank Ray Blundell, Bob Calder, Paul Jaminet, Dan Oberlander, Edward Tong for helpful discussions and assistance.

References

Hills, R. 1986, Memo ASR/MT/T/1015

Hills, R. & Lasenby, A. 1988, presented at the 11th Estec Antenna Workshop on Antenna Measurements, Gothenburg, Sweden

Lesurf, L. 1990, Millimeter-Wave Optics, Devices & Systems (Adam Hilger: New York)

Masson, C. 1991, SMA technical memo No. 50

Morris, D. 1985, IEEE Trans. Ap-33, 749

Zhang, X. 1995, SMA Techical memo, No. 86